

Expression and Iron-Dependent Regulation of Succinate Receptor GPR91 in Retinal Pigment Epithelium

Jaya P. Gnana-Prakasam,^{1,2} Sudha Ananth,¹ Puttur D. Prasad,¹ Ming Zhang,³ Sally S. Atherton,^{2,3} Pamela M. Martin,^{1,2} Sylvia B. Smith,^{2,3} and Vadivel Ganapathy^{1,2}

PURPOSE. GPR91, a succinate receptor, is expressed in retinal ganglion cells and induces vascular endothelial growth factor (VEGF) expression. RPE also expresses VEGF, but whether this cell expresses GPR91 is not known. Excessive iron is also proangiogenic, and hemochromatosis is associated with iron overload. Therefore, we examined the expression and iron-dependent regulation of GPR91 in the RPE.

METHODS. GPR91 expression was examined by RT-PCR and immunohistochemistry. Hemochromatosis mice, cytomegalovirus (CMV) infection of retina, expression of CMV-US2 in RPE, and exposure of RPE to ferric ammonium citrate (FAC) were used to examine the iron-dependent regulation of GPR91 expression. VEGF expression was quantified by qPCR. Knockdown of GPR91 in ARPE-19 cells was achieved with shRNA.

RESULTS. GPR91 was expressed in RPE but only in the apical membrane. Retinal expression of GPR91 was higher in hemochromatosis (*Hfe*^{-/-}) mice than in wild-type (WT) mice. Primary RPE cells from *Hfe*^{-/-} mice had increased GPR91 expression compared with WT RPE cells. Iron accumulation in cells induced by CMV infection, expression of CMV-US2, or treatment with FAC increased GPR91 expression. VEGF expression in the *Hfe*^{-/-} mouse retina was increased at ages younger than 18 months, but the expression was downregulated at older ages. The involvement of GPR91 in succinate-induced expression of VEGF in RPE cells was confirmed with GPR91-specific shRNA.

CONCLUSIONS. GPR91 is expressed in the RPE with specific localization to the apical membrane, indicating that succinate in the subretinal space serves as the GPR91 agonist. Excessive iron in the retina and RPE enhances GPR91 expression; however, VEGF expression does not always parallel GPR91 expression. (*Invest Ophthalmol Vis Sci.* 2011;52:3751-3758) DOI:10.1167/iovs.10-6722

Hereditary hemochromatosis is caused primarily by mutations in *HFE*, which encodes an HLA-like protein involved in iron (*FE*) homeostasis.¹⁻⁴ Iron overload in patients with *HFE* mutations is an age-dependent process; therefore, hemochromatosis as a clinical disease resulting from iron-induced oxidative damage manifests only in persons older than 50 years of

age. Hemochromatosis is an autosomal recessive disorder with a prevalence of homozygosity of approximately 1 in 300 Caucasians. A loss-of-function mutation (Cys282→Tyr282) in *HFE* is responsible for approximately 85% of cases of hemochromatosis.⁵ The clinical features of the disease include cirrhosis, hepatocarcinoma, diabetes, cardiomyopathy, nephropathy, and pituitary dysfunction.¹⁻⁴ *HFE* is necessary for the expression of the iron-regulatory hormone hepcidin in the liver, and the *HFE*-dependent regulation of hepcidin expression is altered in response to the body's iron status.¹⁻⁴ This hormone binds to ferroportin, an iron exporter, and facilitates its degradation. In hemochromatosis, loss of *HFE* function results in decreased production of hepcidin and, hence, in increased density of ferroportin in the basolateral membrane of the intestinal absorptive cells. As a result, iron absorption in the intestine occurs at an increased rate without the *HFE*-mediated feedback control. Enhanced iron absorption increases the levels of iron-bound transferrin in the circulation, which then increases the entry of iron into various tissues through TfR1.

The relevance of hemochromatosis to retinal iron homeostasis had not received much attention until recently because no information was available in the literature on the expression of *HFE* in this tissue. We have shown recently that *HFE* is indeed expressed in the retina, where its expression is restricted to the basolateral membrane of RPE.⁶ Given that RPE functions as a gatekeeper for the entry of nutrients, including iron, from choroidal blood into the neural retina, our findings suggested that *HFE* in RPE may play a critical role in retinal iron homeostasis. Subsequent studies using the *Hfe*^{-/-} mouse model of hemochromatosis have shown that, like the liver, heart, kidney, and pancreas, the retina is also a target organ for iron overload in hemochromatosis.⁷ Excessive iron accumulation in hemochromatosis mice leads to significant morphologic changes throughout the retina in an age-dependent manner. In the RPE, iron accumulation causes hypertrophy and hyperplasia. Studies have shown that the retina expresses not only *HFE* but also other proteins critical for iron homeostasis.⁸⁻¹⁰ Oxidative stress, iron accumulation, and hypertrophy and hyperplasia of RPE are all hallmarks of age-related macular degeneration, another age-dependent disease.¹¹⁻¹⁵ This suggests that hemochromatosis may contribute to the pathogenesis of AMD. In support of this notion, various mouse models of excessive iron accumulation in the retina, including *Hfe*^{-/-} mice and hepcidin knockout mice, have provided evidence of AMD-like morphologic changes in the retina.^{7,14,15}

GPR91 is a G-protein-coupled receptor for succinate.¹⁶ The citric acid cycle intermediate succinate, normally present within mitochondria, is released into the extracellular medium if there is a loss in the balance of local tissue energy demand and supply.¹⁷ The extracellular succinate then serves as an agonist for GPR91. In the kidney, succinate-induced activation of GPR91 regulates the renin-angiotensin system.^{18,19} GPR91 is also expressed in retinal ganglion cells, where it plays a different role.²⁰ Succinate-GPR91 signaling in retinal ganglion cells

From the Departments of ¹Biochemistry and Molecular Biology and ²Cellular Biology and Anatomy and the ³Vision Discovery Institute, Medical College of Georgia, Augusta, Georgia.

Supported by National Eye Institute Grant EY019672.

Submitted for publication October 14, 2010; revised January 23, 2011; accepted February 2, 2011.

Disclosure: **J.P. Gnana-Prakasam**, None; **S. Ananth**, None; **P.D. Prasad**, None; **M. Zhang**, None; **S.S. Atherton**, None; **P.M. Martin**, None; **S.B. Smith**, None; **V. Ganapathy**, None

Corresponding author: Vadivel Ganapathy, Department of Biochemistry and Molecular Biology, Medical College of Georgia, Augusta, GA 30912; vganapat@mcg.edu.

stimulates the expression and secretion of vascular endothelial growth factor (VEGF). This was the first report of the proangiogenic function of GPR91. The same study showed that succinate-GPR91 signaling is a potent mediator of angiogenesis in the normal retina and in diseases associated with retinopathy. RPE also expresses VEGF, but whether this cell expresses GPR91 is not known. Excessive iron is proangiogenic,²¹ and hemochromatosis is associated with iron overload in the retina. Therefore, we examined whether GPR91 is expressed in the RPE and whether the expression is regulated by iron. Infection with cytomegalovirus (CMV) causes iron accumulation in infected cells.²² This is mediated by the protein product of one of the genes in the ultra-specific region of the CMV genome known as US2. US2 causes iron accumulation in infected cells by depleting HFE by proteasomal degradation.^{23,24} Because of this similarity between hemochromatosis and CMV infection, we also studied GPR91 expression in the CMV-infected mouse retina.

MATERIALS AND METHODS

Materials

Reagents were obtained from the following sources: reagent for RNA preparation (TRIzol; Invitrogen-Gibco Corp., Grand Island, NY) and DMEM/F12 culture medium (Invitrogen-Gibco Corp.), RT-PCR kit (Applied Biosystems, Inc., Foster City, CA), and *Taq* polymerase kit (TaKaRa, Tokyo, Japan). Rabbit polyclonal anti-GPR91 and chicken anti-MCT1 were from Alpha Diagnostic International (San Antonio, TX); goat anti-rabbit IgG coupled to Alexa Fluor 568, goat anti-chicken IgG coupled to Alexa Fluor 568, and goat anti-rabbit IgG coupled to Alexa Fluor 488 were from Molecular Probes (Carlsbad, CA).

Animals

C57BL/6 mice were used for the preparation of total RNA from neural retina and RPE/eyecup. Breeding pairs of *Hfe*^{+/-} mice were obtained from the Jackson Laboratory (Bar Harbor, ME). Albino Balb/c mice were used for immunofluorescence analysis and for supraciliary injection of MCMV to induce eye infection. Mice were purchased from Harlan-Sprague-Dawley, Inc. (Indianapolis, IN). All procedures involving mice were approved by the Institutional Committee on Animal Use for Research and Education and were performed in accordance with the ARVO Statement for the Use of Animals in Ophthalmic and Vision Research.

Establishment of Mouse Primary RPE Cell Cultures

Age-matched WT and *Hfe*^{-/-} mice were obtained from the same litter originating from the mating of heterozygous mice. Three-week-old mice were used to establish primary cultures of RPE, as described previously.⁸

Ocular Infection with MCMV

The murine cytomegalovirus (MCMV) (k181 strain) stocks were prepared from salivary gland homogenates of Balb/c mice, as described previously.⁹ Mice were anesthetized by intramuscular injection of a mixture of 42.9 mg/mL ketamine, 8.57 mg/mL xylazine, and 1.43 mg/mL acepromazine at a dose of 0.5 to 0.7 mL/kg body weight. The left eyes of mice were injected with 5×10^3 PFUs of MCMV (or PBS in control mice) in a volume of 2 μ L by way of the supraciliary route, as previously described.⁹

Preparation of Retinal Tissues for Immunostaining and RNA Isolation

Eyes were embedded in OCT compound and frozen at -30°C . Sections (8- μ m thick) were used for immunostaining. For preparation of RNA from posterior segments, corneas and lenses were removed using a

stereomicroscope, and the posterior cup with retina was collected for RNA preparation. In some experiments, the neural retina was peeled from the eyecup, thus leaving behind the RPE/eyecup; RNA was prepared from the neural retina and RPE/eyecup.

RT-PCR and Real-Time PCR

RT-PCR was carried out under optimal conditions specific for PCR primer pairs. The following primers were used: mouse GPR91 forward primer 5'-TGTGAGAATTGGTTGGCAACAG-3' and reverse primer 5'-TCGGTCCATGCTAATGACAGTG-3'; CMV US2 forward primer 5'-GGGAATTCGAGCTCGGTAC-3' and reverse primer 5'-GCTATGAC-CATGATTACGCCAA-3'. Primers for mouse angiopoietin-1 were 5'-GCCTGGATTTCCAGAGGGGCTGG-3' (forward) and 5'-GGGCCG-GATCATCATGGTGGTGG-3' (reverse). Primers for mouse angiopoietin-2 were 5'-GGGGAGAAGAGAAGAGAAGAG-3' (forward) and 5'-CACGGCATTGGACATGTA-3' (reverse). The molecular identity of the PCR products was confirmed by sequencing. HPRT1 mRNA or 18S mRNA was used as the internal control for PCR reaction. Each PCR experiment was repeated at least three times with similar results. Expression levels of target mRNA were quantified by densitometry and normalized with the corresponding internal control.

The following primers were used for quantification of VEGF mRNA in mouse retina by real-time PCR: forward primer 5'-CCTCCT-CAGGGTTTCGGGAACCA-3' and reverse primer 5'-ACCCAAAGT-GCTCCTCGAAGGATC-3'. Real-time amplifications, using detection chemistry (SYBR Green; Applied Biosystems), were run in triplicate on 96-well reaction plates.

Bioluminescence Resonance Energy Transfer Assay

This assay monitors the dissociation of G-protein heterotrimers on the activation of GPR91 with an agonist.^{25,26} HEK293 cells were transfected overnight with human GPR91 cDNA along with constructs coding for G α 1, venus-G β 1, venus-G γ 2, and GRK3 (G-protein-coupled receptor kinase 3)-C terminus-luciferase. Cells were then harvested in PBS containing 5 mM EDTA. Cell suspension was transferred to a 96-well plate (100 μ L/well) and exposed to various intermediates of the citric acid cycle at different concentrations. The luciferase substrate benzyl coelenterazine (5 μ M) was then added to the wells in the dark. Steady state bioluminescence resonance energy transfer (BRET) measurements were made within 15 minutes of exposure of the cell suspensions to ligands using a photon-counting multimode plate reader (Mithras LB940; Berthold Technologies GmbH, Bad Wildbad, Germany). The BRET signal was calculated as the ratio of the emission intensity at 520 to 545 nm to the emission intensity at 475 to 495 nm.

Immunofluorescence Analysis

Retinal sections, fixed in 4% paraformaldehyde and blocked with 1 \times power block, were incubated overnight at 4°C with one or more of the following primary antibodies: polyclonal anti-GPR91 (1:100) and chicken anti-MCT1 (1:1000), either independently or together. Negative controls involved omission of the primary antibodies. Sections were rinsed and incubated for 1 hour with goat anti-rabbit IgG coupled to Alexa Fluor 568, goat anti-chicken IgG coupled to Alexa Fluor 568, and goat anti-rabbit IgG coupled to Alexa Fluor 488, either independently or together as needed. Coverslips were mounted after staining with Hoechst nuclear stain, and sections were examined with a wide-field epifluorescence microscope (Carl Zeiss, Oberkochen, Germany). Polarized expression of GPR91 in RPE with MCT1 as a specific marker of the apical membrane was investigated by double-labeling, and the slides were examined by laser-scanning confocal microscopy. Immunohistochemistry studies were repeated twice, and the results from these two experiments were similar.

Transient Transfection of Lentivirus-CMV-US2 Construct

CMV-US2 cDNA was prepared by PCR. A plasmid (pAdtet7) containing human CMV US2 cDNA insert was kindly provided by David C. Johnson (Department of Molecular Microbiology and Immunology, Oregon Health and Science University, Portland, OR). The cDNA insert was amplified from the plasmid using the following primers: 5'-GGGAATTCGAGCTCGGTAC-3' (forward) and 5'-GCTATGACCATGATACGCCAA-3' (reverse). The product was sequenced to confirm its molecular identity and then subcloned into the lentiviral vector pLKO1. This plasmid was used to transiently transfect primary mouse RPE cells and human ARPE-19 cells. Recombinant lentivirus was produced by cotransfection into 293FT cells with CMV-US2 cDNA in lentiviral pLKO1 vector and three other helper vectors—pLP-1, pLP-2, and pVSVG (Invitrogen)—using transfection reagent (Lipofectamine 2000; Invitrogen). Lentiviral supernatants were harvested at 72 hours after transfection and were filtered through a 0.45- μ m membrane. Cells were infected for 24 hours with fresh lentivirus expressing either the control vector or CMV-US2 in medium containing 8 μ g/mL polybrene and were cultured for an additional 48 hours. After transfection, cells were washed with PBS, and RNA or protein was isolated for RT-PCR and Western blot analysis, respectively.

Western Blot Analysis

Protein lysates were subjected to SDS-PAGE using 10% polyacrylamide gel. The proteins were then transferred onto a polyvinylidene fluoride membrane and probed with specific antibodies. Positive bands were detected with appropriate secondary antibodies coupled to horseradish peroxidase. Signals were developed with an enhanced chemiluminescence detection kit. β -Actin was used as the internal control. The levels of target protein were quantified by densitometry and normalized with the corresponding internal control. Western blot analysis was repeated twice with comparable results.

Treatment of RPE Cells with Ferric Ammonium Citrate

Primary RPE cells and human RPE cell lines ARPE-19 and HRPE were seeded in 24-well culture plates and cultured for 24 hours. Fresh culture medium was then added to cells with or without ferric ammonium citrate (FAC) (100 μ g/mL), and the cells were cultured for an additional 72 hours. Cells were then used for RNA extraction. The concentration of FAC and the treatment time were selected based on published reports to cause iron overload in cells for optimal iron-induced gene expression changes.²⁷ We used these conditions in RPE cells to demonstrate iron-induced changes in the expression of the cystine/glutamate exchanger and ferroportin.^{7,28}

shRNA-Induced Silencing of GPR91 in ARPE-19 Cells

Lentiviral-based shRNAs were used to knock down GPR91 in ARPE-19 cells. We generated stable cell lines of ARPE-19 with GPR91 knockdown using gene-specific shRNA constructs with the lentivirus plasmid vector pLKO.1-puromycin (Open Biosystems, Huntsville, AL). The following four constructs were used: shRNA1 (clone TRCN0000008975), shRNA2 (clone TRCN0000008976), shRNA3 (clone TRCN0000008977), and shRNA4 (clone TRCN0000008978). Stable cell lines were generated by infecting ARPE-19 cells independently with each of the four lentiviral-shRNA constructs and then selecting stable cell lines by puromycin (1 μ g/mL) resistance. A stable cell line with a lentiviral vector only, without the shRNA, was used as the negative control. Knockdown of GPR91 expression was verified by RT-PCR. The sequences of shRNAs are as follows: CCGGGCTCTGCATAAGCAACCGATACTCGAGTATCGGTTGCTTATGCA-GAGCTTTTT (shRNA1); CCGGGCCTCTCAACTTGGTCATCATCTC-GAGATGATACCAAGTTGAG AGGCTTTTT (shRNA2); CCGGGCGGCTA-CATCTTCTCTGAACTCGAGTTCAGAGA GAAGATGTAGCCGTTTTT

(shRNA3); CCGGCCCATGCTGATAAGGAGTTATCTCGAG ATAACCTCCTT ATCAGCATGGGTTTTT (shRNA4).

RESULTS

Expression and Localization of GPR91 in Retina

To investigate the expression pattern of GPR91 in the mouse retina, RT-PCR was performed using RNA isolated from the neural retina (mostly devoid of RPE) and the RPE/eyecup of normal mouse. We found evidence for the expression of GPR91 mRNA in the RPE/eyecup as well as in the neural retina (Fig. 1A). Expression was considerably higher in the RPE/eyecup than in the neural retina. Immunofluorescence analysis of GPR91 protein showed positive signals throughout the retina, including the RPE cell layer (Fig. 1B). Negative controls with omission of the primary antibody did not yield positive signals. To determine whether GPR91 is expressed in RPE in a polarized manner, double-labeling studies were performed with a rabbit polyclonal anti-GPR91 antibody and a chicken polyclonal anti-MCT1 antibody. MCT1 is a marker for the apical membrane in RPE.²⁹ Laser-scanning confocal microscopic analysis of the immunostained retinal sections revealed that GPR91 (green) and MCT1 (red) were both colocalized in the apical membrane of RPE (Fig. 1C).

Succinate as a GPR91 Agonist

The activation of GPR91 by succinate was monitored using the BRET assay. We coexpressed human GPR91 and human G_{i1} in HEK293 cells along with Venus1-155- G_{i2} and Venus155-239- G_{i1} constructs. When GPR91 is activated with an agonist, G_{i2} dimer containing the complementary fragments of the yellow fluorescent protein venus (the 1- to 155-amino acid fragment and the 155- to 239-amino acid fragment) dissociates from G_{i1} . The dimer then binds to the GRK3-C terminus-luciferase fusion protein, enabling BRET in the presence of benzyl coelenterazine, a substrate for luciferase. Using this technique, we were able to show that succinate is an effective agonist for GPR91 (data not shown). The value for ED_{50} (i.e., the concentration necessary for half-maximal activation of the receptor) was 91 ± 14 μ M. We also tested other citric acid cycle intermediates for their ability to activate GPR91. None of the compounds tested (citrate, fumarate, malate, or α -ketoglutarate) was able to serve as an agonist for GPR91 (data not shown), demonstrating that succinate is a specific ligand for this receptor. The activation of GPR91 by succinate has been demonstrated previously based on changes in the secretion of prostaglandin E2 or forskolin-induced cAMP levels.^{16,18} The present studies demonstrate for the first time the dynamics of the individual components of the trimeric G-protein complex during receptor activation.

Expression of GPR91 in Hemochromatosis Mouse (*Hfe*^{-/-}) Retina

To determine whether GPR91 expression is altered in the RPE in hemochromatosis, RT-PCR was carried out using RNA from primary cultures of WT and *Hfe*^{-/-} RPE cells. These studies showed that GPR91 mRNA levels were higher in primary RPE cells from *Hfe*^{-/-} mice than from WT mice (Fig. 2A). Because the receptor is expressed not only in RPE cells but also in other retinal cell types, we analyzed the expression of GPR91 protein by Western blot in whole retinas from WT and *Hfe*^{-/-} mice. The levels of the receptor protein were increased in the retinas of hemochromatosis mice (Fig. 2B). These results were corroborated by immunohistochemistry with retinal sections. Both in 8-month-old mice and in 18-month-old mice, the GPR91-spe-

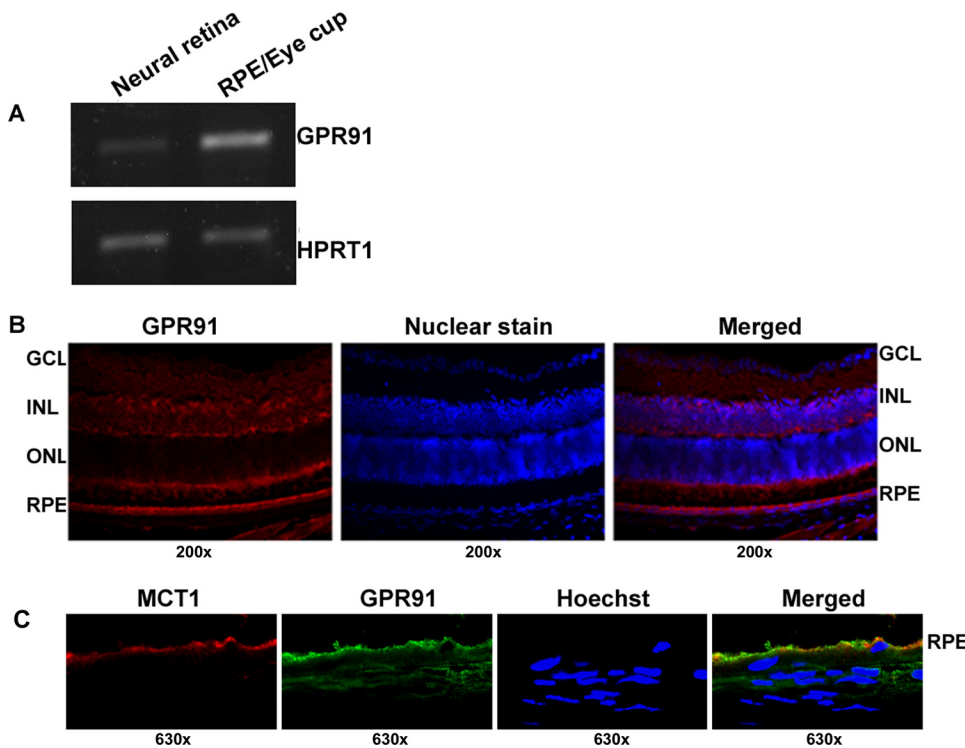


FIGURE 1. Expression and localization of GPR91 in mouse retina. (A) RT-PCR analysis of GPR91 mRNA in neural retina and RPE/eyecup. HPRT1 was used as an internal control. (B) Immunofluorescence localization of GPR91 protein in mouse retina. *Left:* staining in the retina using GPR91 primary antibody; *middle:* nuclear staining; *right:* merged image. GCL, ganglion cell layer; INL, inner nuclear layer; ONL, outer nuclear layer; RPE, retinal pigment epithelium. (C) Confocal analysis of the polarized expression of GPR91 in RPE. MCT1 was used as a marker for the RPE apical membrane. GPR91 was detected with a secondary antibody conjugated to Alexa Fluor 488 (green), and MCT1 was detected with a secondary antibody conjugated to Alexa Fluor 568 (red). Hoechst was used as a nuclear stain. Merging of the fluorescent signals in the RPE cell layer indicates the coexpression of the two proteins in RPE apical membrane.

cific signal was higher in the knockout mouse retina than in the age-matched WT mouse retina (Fig. 2C).

Expression of GPR91 in Retina during MCMV Infection In Vivo

GPR91 mRNA levels were increased in whole retina when infected with MCMV (Fig. 3A). We have shown previously that in vitro infection of primary RPE cells and in vivo infection of mouse eyes with MCMV deplete Hfe protein in the retina.⁹ In the present study, the levels of GPR91 protein increased markedly in primary RPE cells in response to MCMV infection in vitro and in the whole retina in response to MCMV infection in vivo (Figs. 3B, 3C).

Regulation of GPR91 Expression in RPE by CMV-US2

Iron accumulation in mammalian cells during CMV infection is mediated by US2 encoded by the viral genome. On infection of the host cell, CMV-US2 binds to newly synthesized HFE and translocates it from the endoplasmic reticulum to the cytosol

for subsequent proteasomal degradation.^{22,23} We have shown previously that CMV infection of RPE and retina in mice leads to Hfe depletion and, consequently, to excessive iron accumulation.⁹ Here we used ectopic expression of CMV US2 in the human RPE cell line ARPE-19 and in mouse primary RPE cells to induce HFE degradation as a means to cause iron overload, mimicking hemochromatosis. Expression of US2 in RPE cells had minimal effect on the steady state levels of HFE mRNA but reduced the steady state levels of HFE protein (Figs. 4A, 4B). Under these conditions, the expression of GPR91 was enhanced, demonstrable both at the mRNA level and the protein level (Figs. 4A, 4B).

Effect of Ferric Ammonium Citrate on GPR91 Expression in RPE

To investigate directly the influence of cellular iron status on the expression of GPR91 in RPE, we exposed mouse primary RPE cells and two human RPE cell lines (ARPE-19 and HRPE) to FAC (100 μ g/mL) for 72 hours to increase cellular iron levels. After the treatment, we monitored GPR91 mRNA levels by

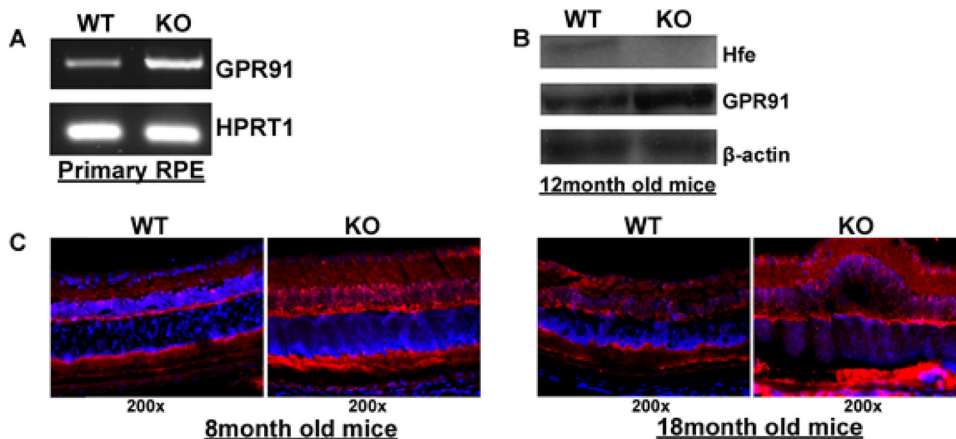


FIGURE 2. Upregulation of GPR91 in retina in an *Hfe*^{-/-} hemochromatosis mouse model. (A) RT-PCR analysis of GPR91 mRNA in WT and *Hfe*^{-/-} (KO) primary RPE cells. HPRT1 was used as an internal control. (B) Western blot analysis of GPR91 protein in whole retinas from WT and *Hfe*^{-/-} (KO) mice. β -Actin was used as an internal control. (C) Immunofluorescence analysis of GPR91 protein in 8-month-old and 18-month-old WT and *Hfe*^{-/-} (KO) mouse retinas.

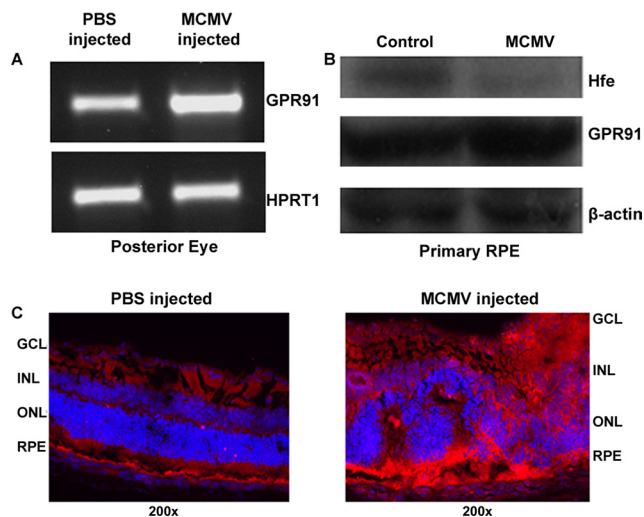


FIGURE 3. Upregulation of GPR91 in CMV-infected mouse retina and RPE cells. (A) Mice were infected in vivo by intraocular injection of MCMV. Control mice were injected with PBS. RT-PCR was performed for GPR91 with RNA samples from whole retinas of PBS-injected and MCMV-injected mice. HPRT1 was used as an internal control. (B) Primary mouse RPE cells were infected in vitro with MCMV, and the levels of GPR91 protein were analyzed by Western blot in control and MCMV-infected cells. β -Actin was used as an internal control. (C) Mice were infected in vivo by intraocular injection of MCMV. Control mice were injected with PBS. Retinal sections were prepared on day 7 after infection and used for immunofluorescence detection of GPR91 protein.

RT-PCR. In each case, exposure to FAC increased the levels of GPR91 mRNA (Fig. 5).

Expression of VEGF and Other Proangiogenic Factors in Wild-type and *Hfe*^{-/-} Mice

GPR91-succinate signaling is proangiogenic in the retina and is associated with increased expression of VEGF, angiopoietin-1, and angiopoietin-2.²⁰ Here we have demonstrated that excessive iron accumulation in retina increases GPR91 expression. In addition, we have shown recently that iron accumulates excessively in the retina in the *Hfe*^{-/-} hemochromatosis mouse model and that significant morphologic changes in the iron-overloaded retina occur in an age-dependent manner.⁷ Based on these findings, we asked whether the expression of proangiogenic factors (VEGF, Ang-1, and Ang-2) is altered in the whole retina of the *Hfe*^{-/-} hemochromatosis mice. We found an age-dependent effect of *Hfe* deletion on mRNA levels for VEGF, Ang-1, and Ang-2 in the mouse retina. When the animals were 8 months old and 18 months old, mRNA levels for these proangiogenic factors were markedly higher in *Hfe*^{-/-} mouse retinas than in WT mouse retinas (Fig. 6). In contrast, the expression of all three factors was drastically decreased in whole retinas in 24-month-old *Hfe*^{-/-} mice compared with age-matched WT mouse retinas, despite the fact that GPR91 expression remained elevated at this age (Fig. 6).

Involvement of GPR91 in Succinate-Induced Expression of VEGF in Iron-Overloaded ARPE-19 Cells

To demonstrate unequivocally the involvement of GPR91 in VEGF expression in the iron-overloaded RPE, we compared the effects of FAC and succinate on VEGF mRNA between ARPE-19 cells with normal expression of GPR91 and ARPE-19 cells with shRNA-mediated knockdown of GPR91. Among the four GPR91-specific shRNAs used, two shRNAs (shRNA2 and

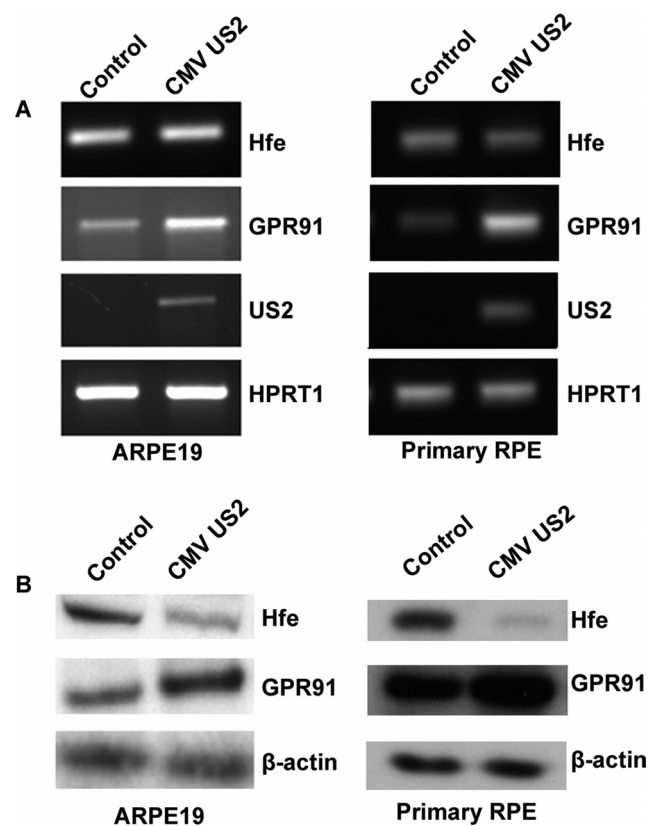


FIGURE 4. Upregulation of GPR91 in mouse and human RPE cells by CMV-US2. (A) RT-PCR analysis of *Hfe*, GPR91, CMV-US2, and HPRT1 with RNA from control RPE cells (ARPE-19 cells and primary mouse RPE cells) and from RPE cells treated with lentivirus carrying the *CMV-US2* gene. HPRT1 was used as an internal control. (B) Western blot using protein lysates from control RPE cells and from RPE cells treated with lentivirus carrying the *CMV-US2* gene. The blots were developed using primary antibody specific to *Hfe* or GPR91. β -Actin was used as an internal control.

shRNA3) showed marked knockdown of GPR91 expression (Fig. 7A). In control ARPE-19 cells, treatment with FAC (100 μ g/mL; 72-hour treatment) and succinate (2 mM; the final 16 hours of the 72-hour FAC treatment) increased the expression of VEGF mRNA; this effect was abolished in ARPE-19 cells with shRNA-mediated GPR91 knockdown (Fig. 7B). These results demonstrate that GPR91 mediates the succinate-induced expression of VEGF in iron-overloaded RPE cells.

DISCUSSION

The present studies provide novel information regarding the expression of the succinate receptor GPR91 in mouse retina.

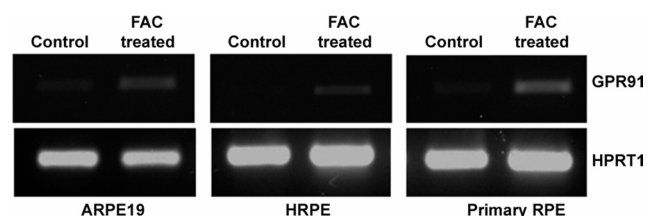


FIGURE 5. Upregulation of GPR91 in mouse and human RPE cells by treatment with FAC. Human RPE cell lines ARPE-19 and HRPE and mouse primary RPE cells were treated with or without FAC (100 μ g/mL) for 72 hours. RNA prepared from these cells was used for RT-PCR analysis of GPR91 mRNA with HPRT1 as an internal control.

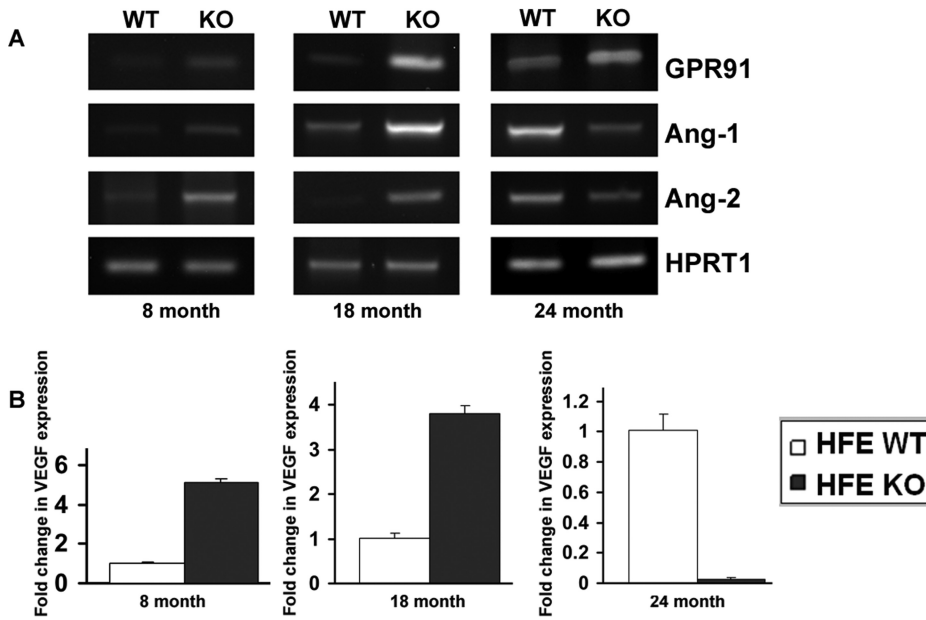


FIGURE 6. Expression of proangiogenic factors VEGF, angiopoietin-1 (Ang-1), and angiopoietin-2 (Ang-2) in retina in WT and *Hfe*^{-/-} (KO) mice. RNA was isolated from whole retinas of 8-month-old, 18-month-old, and 24-month-old WT mice and *Hfe*^{-/-} mice. mRNA levels for GPR91, Ang-1, and Ang-2 were determined by RT-PCR, with HPRT1 as an internal control (A). VEGF mRNA levels were determined by real-time PCR (B). Three RNA samples from three mice for each genotype and age were used. Data for the real-time PCR are presented as the mean ± SE for the three independent RNA samples.

We have shown here for the first time that the receptor is expressed in RPE. The expression of GPR91 has been demonstrated recently in retinal ganglion cells,²⁰ but its expression in RPE was not known. Even more novel and important is the finding that the receptor is expressed in this cell layer only in the apical membrane and not in the basolateral membrane. Because the apical membrane faces the neural retina whereas the basolateral membrane is in contact with choroidal blood, the polarized expression of GPR91 in the apical membrane suggests that the receptor is activated by succinate present in the subretinal space rather than by succinate present in blood. Another important outcome of the present studies is the observation that the expression of the receptor is regulated by

the iron status within the retina. Excessive iron accumulation in the retina, caused either by the deletion of *Hfe* or by infection of the retina by CMV, upregulates GPR91 expression. This iron-dependent regulation is observed not only in RPE but also in other cell types within the retina. This represents the first report on the regulation of GPR91 expression by iron in any tissue.

These results have significant clinical relevance. Loss-of-function mutations in HFE in humans lead to hemochromatosis, a disease associated with excessive iron accumulation in various systemic organs. We have shown recently, using the *Hfe*^{-/-} mouse as an animal model for hemochromatosis, that the retina is also a target organ for iron accumulation in this

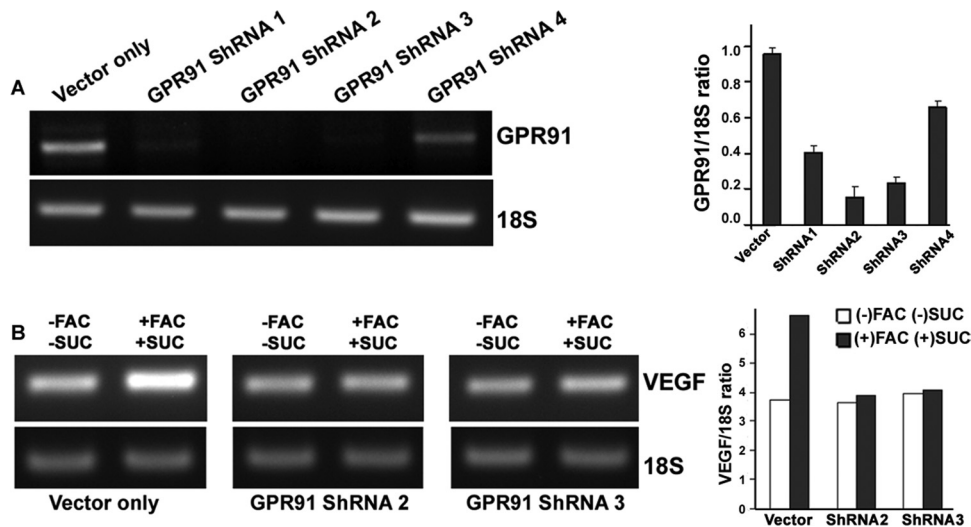


FIGURE 7. Induction of VEGF mRNA expression by FAC and succinate in ARPE-19 cells with or without GPR91 knockdown. (A) ARPE-19 cells were subjected to lentivirus-mediated knockdown of GPR91 expression with four different gene-specific shRNAs. The magnitude of knockdown was monitored by RT-PCR, with 18S RNA as an internal control. Data (normalized to the internal control) are presented as mean ± SE from three RNA preparations. (B) Control ARPE-19 cells (vector only) and shRNA-expressing ARPE-19 cells were treated with FAC (100 μg/mL) for 72 hours; the final portion, 16 hours, of this 72-hour period occurred with or without succinate (2 mM). RNA from the cells with and without the treatment was used for RT-PCR to analyze the levels of VEGF mRNA. 18S RNA was used as an internal control. Data (normalized to the internal control) are presented as the average of two independent experiments.

disease.⁷ The retina has generally been thought to be immune to changes in circulating levels of iron, implying that the iron status of this organ is not likely to be affected in hemochromatosis. Our findings in the mouse model of hemochromatosis dispel this notion. The results of the present studies showing that retinal expression of GPR91 is upregulated by iron overload have direct relevance to patients with hemochromatosis. Excessive iron accumulation is also a hallmark of cells infected with CMV.²²⁻²⁴ On the mechanistic level, there is a similarity in tissue iron accumulation between hemochromatosis and CMV infection. Excessive iron accumulation in tissues in the most prevalent form of hemochromatosis in humans occurs as a consequence of loss-of-function mutations in HFE. The Cys282→Tyr282 mutation in HFE is responsible for >85% cases of hemochromatosis in humans. This mutation interferes with the association of HFE with its partner β 2-microglobulin, consequently leading to the failure of HFE recruitment to the plasma membrane and hence to accelerated degradation.³⁰ This loss of HFE in the plasma membrane is responsible for the dysregulation of iron handling in various tissues, with an ultimate end result of excessive iron in circulation. A situation similar to this phenomenon underlies iron accumulation in CMV-infected cells. One of the proteins encoded by the CMV genome, US2, promotes the degradation of HFE in infected cells, resulting in the loss of the protein in the plasma membrane. We have previously reported that retinal CMV infection in mice leads to the degradation of Hfe in RPE, causing iron accumulation within the retina.⁹ In the present study, we have shown that CMV infection of the mouse retina *in vivo* or exogenous expression of CMV-US2 in RPE cells leads to the upregulation of GPR91. These findings are important because CMV infection is one of the major causes of retinitis in immunocompromised persons, resulting in serious visual deficits.³¹ Iron is a pro-oxidant, and excessive accumulation of iron may lead to oxidative stress and tissue damage. Iron overload resulting from a variety of causes is associated with significant morphologic changes in the retina.¹¹⁻¹³ Excessive iron as an oxidant is an important pathologic factor not only in hemochromatosis and CMV infection but also in other diseases such as AMD. Recent studies³²⁻³⁴ have shown that iron-induced oxidative stress plays a role in the pathophysiology of AMD.

The recent report by Sapieha et al.,²⁰ which describes the expression of GPR91 in retinal ganglion cells, has provided unequivocal evidence for a proangiogenic role of this receptor. Activation of the receptor in ganglion cells by its agonist succinate stimulates the synthesis and secretion of the proangiogenic molecules VEGF, angiopoietin-1, and angiopoietin-2. This is accompanied by enhanced retinal angiogenesis. This report also has provided evidence of a critical role for GPR91-succinate signaling in the normal development of the retinal vasculature. In addition to this normal physiological function, the signaling pathway seems to contribute to angiogenesis associated with pathologic conditions such as proliferative ischemic retinopathy. Using a mouse model of oxygen-induced retinopathy, the authors of the report showed that the levels of succinate increase approximately threefold in ischemic retinas. Even though there is no change in the expression levels of GPR91, the increase in the agonist levels is sufficient to activate the signaling pathway, leading to the increased secretion of proangiogenic factors and, consequently, to the promotion of pathologic vasculogenesis.

In contrast to what was found in ischemic retinas,²⁰ the present study shows that excessive iron accumulation in the retina, caused either by *Hfe* deletion or by CMV infection, increases GPR91 expression. This upregulation occurs not only in RPE but also in other retinal cell types. In hemochromatosis mice, this phenomenon is associated with the increased expression of VEGF, angiopoietin-1, and angiopoietin-2 *in vivo*

when the animals are 18 months of age and younger, apparently indicating the stimulation of receptor signaling. However, the expression of these proangiogenic factors decreased dramatically in 24-month-old hemochromatosis mice in spite of the continued upregulation of GPR91. The reasons for this age-dependent difference and the *in vivo* relevance of these findings to retinal pathology are not known at present and remain to be determined. We were unable to measure succinate levels in mouse retinas; therefore, we do not know at this time whether the agonist levels are also altered in hemochromatosis mice. Recently, it was reported that increased iron availability in lens epithelial cells decreases nuclear translocation of hypoxia-inducible factor 1- α , a transcription factor that regulates many genes, including VEGF.³⁵ This study showed that iron depletion results in increased VEGF levels by stabilizing HIF-1 α . These findings are different from our present studies in the retina. Given that we do not know whether lens epithelial cells express GPR91, additional studies are needed to determine whether the effects of iron on VEGF secretion by GPR91-succinate signaling could be cell type-specific.

GPR91 in the retina and its regulation by iron are also likely to be important in diabetic retinopathy. There is substantial evidence for a positive correlation between iron levels in the body and diabetes.³⁶⁻³⁸ In diabetic retina, iron homeostasis is disrupted, thus leading to iron overload. Whether the excessive iron accumulation seen in diabetic retina is a cause or a consequence is debatable; however, the observations that insulin, oxidative stress, and inflammatory cytokines influence iron homeostasis suggest that iron accumulation in the retina is likely to be a consequence of diabetes because this disease is also associated with the loss of insulin action, chronic inflammation, and increased generation of reactive oxygen and nitrogen species. No information is available in the literature regarding whether succinate levels are altered in diabetic tissues. Succinate is an intermediate in the citric acid cycle, and aconitase, a mitochondrial enzyme in the metabolic pathway, is activated by iron.²⁷ Similarly, the cytosolic isoform of aconitase is activated by iron. Therefore, it seems plausible that excessive iron accumulation associated with diabetes may elevate succinate levels in tissues. This is only speculative at this time but the possibility merits further investigation.

Acknowledgments

The authors thank Penny Roon (Histology Core, Medical College of Georgia) for preparation of the retinal sections.

References

1. Wrighting DM, Andrews NC. Iron homeostasis and erythropoiesis. *Curr Top Dev Biol.* 2008;82:141-167.
2. Fleming RE, Britton RS, Waheed A, Sly WS, Bacon BR. Pathophysiology of hereditary hemochromatosis. *Semin Liver Dis.* 2005;25:411-419.
3. Beutler E. Hemochromatosis: genetics and pathophysiology. *Annu Rev Med.* 2006;57:331-347.
4. Fleming RE, Britton RS. Iron imports, VI: HFE and regulation of intestinal iron absorption. *Am J Physiol Gastrointest Liver Physiol.* 2006;290:G590-G594.
5. Feder JN, Gnirke A, Thomas W, et al. A novel MHC class I-like gene is mutated in patients with hereditary haemochromatosis. *Nat Genet.* 1996;13:399-408.
6. Martin PM, Gnana-Prakasam JP, Roon P, Smith RG, Smith SB, Ganapathy V. Expression and polarized localization of the hemochromatosis gene product HFE in the retinal pigment epithelium. *Invest Ophthalmol Vis Sci.* 2006;47:4238-4244.
7. Gnana-Prakasam JP, Thangaraju M, Liu K, et al. Absence of iron-regulatory protein HFE results in hyper-proliferation of retinal pigment epithelium mediated by induction of cystine/glutamate transporter. *Biochem J.* 2009;424:243-252.

8. Gnana-Prakasam JP, Martin PM, Mysona BA, Roon P, Smith SB, Ganapathy V. Hepsidin expression in mouse retina and its regulation via lipopolysaccharide/Toll-like receptor-4 pathway independent of Hfe. *Biochem J.* 2008;411:79–88.
9. Gnana-Prakasam JP, Martin PM, Zhang M, Atherton SS, Smith SB, Ganapathy V. Expression of the iron-regulatory protein hemojuvelin in retina and its regulation during cytomegalovirus infection. *Biochem J.* 2009;419:533–543.
10. Hahn P, Dentchev T, Qian Y, Rouault T, Harris ZL, Dunaief JL. Immunolocalization and regulation of iron handling proteins ferritin and ferroportin in the retina. *Mol Vis.* 2004;10:598–607.
11. Dunaief JL. Iron-induced oxidative damage as a potential factor in age-related macular degeneration: the Cogan Lecture. *Invest Ophthalmol Vis Sci.* 2006;47:4660–4664.
12. He X, Hahn P, Iacovelli J, et al. Iron homeostasis and toxicity in retinal degeneration. *Prog Retin Eye Res.* 2007;26:649–673.
13. Gnana-Prakasam JP, Martin PM, Smith SB, Ganapathy V. Expression and function of iron-regulatory proteins in retina. *IUBMB Life.* 2010;62:363–370.
14. Hadziahmetovic M, Denntchev T, Song Y, et al. Ceruloplasmin/hephaestin knockout mice model morphologic and molecular features of AMD. *Invest Ophthalmol Vis Sci.* 2008;49:2728–2736.
15. Hadziahmetovic M, Song Y, Ponnuru P, et al. Age-dependent retinal iron accumulation and degeneration in hepcidin knockout mice. *Invest Ophthalmol Vis Sci.* 2011;52:109–118.
16. He W, Miao FJ, Lin DC, et al. Citric acid cycle intermediates as ligands for orphan G-protein-coupled receptors. *Nature.* 2004;429:188–193.
17. Hebert SC. Physiology: orphan detectors of metabolism. *Nature.* 2004;429:143–145.
18. Toma I, Kang JJ, Sipsos A, et al. Succinate receptor GPR91 provides a direct link between high glucose levels and renin release in murine and rabbit kidney. *J Clin Invest.* 2008;118:2526–2534.
19. Vargas SL, Toma I, Kang JJ, Meer EJ, Peti-Peterdi J. Activation of the succinate receptor GPR91 in macula densa cells causes renin release. *J Am Soc Nephrol.* 2009;20:1002–1011.
20. Sapielha P, Sirinyan M, Hamel D, et al. The succinate receptor GPR91 in neurons has a major role in retinal angiogenesis. *Nat Med.* 2008;14:1067–1076.
21. Coffman LG, Parsonage D, D'Agostino R Jr, Torti FM, Torti SV. Regulatory effects of ferritin on angiogenesis. *Proc Natl Acad Sci USA.* 2009;106:570–575.
22. Drakesmith H, Prentice A. Viral infection and iron metabolism. *Nat Rev Microbiol.* 2008;6:541–552.
23. Arieh SVB, Laham N, Schechter C, Yewdell JW, Coligan JE, Ehrlich R. A single viral protein HCMV US2 affects antigen presentation and intracellular iron homeostasis by degradation of classical HLA class I and HFE molecules. *Blood.* 2003;101:2858–2864.
24. Chevalier MS, Johnson DC. Human cytomegalovirus US3 chimeras containing US2 cytosolic residues acquire major histocompatibility class I and II protein degradation properties. *J Virol.* 2003;77:4731–4738.
25. Hollins B, Kuravi S, Digby GJ, Lambert NA. The C-terminus of GRK3 indicates rapid dissociation of G protein heterotrimers. *Cell Signal.* 2009;21:1015–1021.
26. Singh N, Thangaraju M, Prasad PD, et al. Blockade of dendritic cell development by bacterial fermentation products butyrate and propionate through a transporter (Slc5a8)-dependent inhibition of histone deacetylases. *J Biol Chem.* 2010;285:27601–27608.
27. Juang HH. Modulation of iron on mitochondrial aconitase expression in human prostatic carcinoma cells. *Mol Cell Biochem.* 2004;265:185–194.
28. Chothe PP, Gnana-Prakasam JP, Ananth S, et al. Transport of hepcidin, an iron-regulatory peptide hormone, into retinal pigment epithelial cells via oligopeptide transporters and its relevance to iron homeostasis. *Biochem Biophys Res Commun.* 2011;405:244–249.
29. Philp NJ, Wang D, Yoon H, Hjelmeland LM. Polarized expression of monocarboxylate transporters in human retinal pigment epithelium and ARPE-19 cells. *Invest Ophthalmol Vis Sci.* 2003;44:1716–1721.
30. Waheed A, Parkkila S, Zhou XY, et al. Hereditary hemochromatosis: effects of C282Y and H63D mutations on association with β 2-microglobulin, intracellular processing, and cell surface expression of the HFE protein in COS-7 cells. *Proc Natl Acad Sci USA.* 1997;94:12384–12389.
31. Scholz M, Doerr HW, Cinatl J. Human cytomegalovirus retinitis: pathogenicity, immune invasion and persistence. *Trends Microbiol.* 2003;11:171–178.
32. Hahn P, Milam AH, Dunaief JL. Maculas affected by age-related macular degeneration contain increased chelatable iron in the retinal pigment epithelium and Bruch's membrane. *Arch Ophthalmol.* 2003;121:1099–1105.
33. Dentchev T, Hahn P, Dunaief JL. Strong labeling for iron and the iron-handling proteins ferritin and ferroportin in the photoreceptor layer in age-related macular degeneration. *Arch Ophthalmol.* 2005;123:1745–1746.
34. Wong RW, Richa DC, Hahn P, Green WR, Dunaief JL. Iron toxicity as a potential factor in AMD. *Retina.* 2007;27:997–1003.
35. Harned J, Ferrell J, Lall MM, et al. Altered ferritin subunit composition: change in iron metabolism in lens epithelial cells and downstream effects on glutathione levels and VEGF secretion. *Invest Ophthalmol Vis Sci.* 2010;51:4437–4446.
36. Fernandez-Real J, Lopez-Bermejo A, Ricart W. Cross-talk between iron metabolism and diabetes. *Diabetes.* 2002;51:2348–2354.
37. Rajpathak SN, Crandall JP, Wylie-Rosett J, Kabat GC, Rohan TE, Hu FB. The role of iron in type 2 diabetes in humans. *Biochim Biophys Acta.* 2009;1790:671–681.
38. Ciudin A, Hernandez C, Simo R. Iron overload in diabetic retinopathy: a cause or a consequence of impaired mechanisms? *Exp Diabetes Res.* In press.